PLASTID STATUS INFLUENCES CELL FATE DECISIONS AT THE PLANT SHOOT APEX

Margaret E. Wilson[1], R. Howard Berg[2] and Elizabeth S. Haswell[1]*

[1]Department of Biology, Mailbox 1137, Washington University in Saint Louis, Saint Louis, MO, USA

[2]Donald Danforth Plant Science Center, 975 North Warson Rd., Saint Louis, MO, USA

*Corresponding author

SUMMARY STATEMENT

Plastid osmotic stress influences cell fate decisions at the plant shoot apex via two established mechanisms that control proliferation: the cytokinin/WUSCHEL stem cell identity loop and a plastid-to-nucleus signaling pathway.

ABSTRACT

The balance between proliferation and differentiation in the plant shoot apical meristem is controlled by regulatory loops involving the phytohormone cytokinin and stem cell identity genes. Concurrently, cellular differentiation in the developing shoot is coordinated with the environmental and developmental status of plastids within those cells. Here we employ an *Arabidopsis thaliana* mutant exhibiting constitutive plastid osmotic stress to investigate the molecular and genetic pathways connecting plastid status with cell fate decisions at the shoot apex. *msl2 msl3* mutants exhibit dramatically enlarged and deformed plastids in the shoot apical meristem, and develop a mass of callus tissue at the shoot apex. Callus production in this mutant is characterized by increased cytokinin levels, the down-regulation of cytokinin signaling inhibitors *ARR7* and ARR15, and induction of the stem cell identity gene *WUSCHEL* and is reduced in the absence of the cytokinin receptor AHK2. Furthermore, plastid stress-induced apical callus requires elevated plastidic ROS, ABA biosynthesis, and retrograde signaling proteins GUN1 and ABI4. These results establish a functional link between the cytokinin/WUS pathway and retrograde signaling in controlling cell fate at the shoot apex.

INTRODUCTION

How cell fate is determined is a fundamental question. The development of land plants provides a unique opportunity to study this decision-making process, as plant cell identity is highly plastic (Gaillochet and Lohmann, 2015). A classic illustration of plant cell pluripotency is the ability to produce a mass of undifferentiated cells referred to as callus. Callus results from the reacquisition of an undifferentiated state or the initial inability to differentiate properly, and is generated by a variety of mechanisms which include wounding and exposure to pathogens (Ikeuchi et al., 2013). The best-understood and most widely employed way to induce the production of callus is treatment with two phytohormones, cytokinin (CK) and auxin (Skoog and Miller, 1957).

In addition, land plants maintain the ability to develop new organs continuously during their lifespan. This is made possible by small self-renewing pools of undifferentiated cells, called meristems, from which new organs are derived as the plant grows (Aichinger et al., 2012; Gaillochet and Lohmann, 2015). Above ground, the maintenance and regulation of the shoot apical meristem (SAM) is critical for the proper specification and positioning of leaves (Barton, 2010). SAM identity requires both the imposition of stem cell fate by the WUSCHEL(WUS)/CLAVATA(CLV) signaling circuit (Schoof et al., 2000) (Fletcher et al., 1999) and the suppression of differentiation by SHOOTMERISTEMLESS (STM) (Endrizzi et al., 1996; Long et al., 1996).

CK plays a key role in the function of the SAM. In the central zone (CZ), CK promotes proliferation, while auxin promotes differentiation in the peripheral zone (PZ) (Schaller et al., 2015). Localized CK perception and response specifies the organizing center of the SAM, also the region of *WUS* expression (Chickarmane et al., 2012; Gordon et al., 2009; Zurcher et al., 2013). WUS activity maintains itself through a positive feedback loop involving CK response via Type-A Arabidopsis Response Regulators (ARRs), key negative regulators of CK signaling (Leibfried et al., 2005; Schuster et al., 2014; To et al., 2007; Zhao et al., 2010). In addition, auxin serves to promote CK signaling in the meristem by repressing ARRs (Zhao et al., 2010). Thus, auxin and CK levels interact with the WUS/CLV pathway to regulate the balance between cell differentiation and cell proliferation both in callus and in the SAM (Gaillochet and Lohmann, 2015; Ikeuchi et al., 2013).

Shoot development also depends on plastids, endosymbiotic organelles responsible for photosynthesis, amino acid, starch, and fatty acid biosynthesis and the production of many hormones

and secondary metabolites (Neuhaus and Emes, 2000). Plastids are present in almost every plant cell, and develop specialized characteristics associated with the cell type in which they reside (Jarvis and Lopez-Juez, 2013). As cells leave the SAM and take on the appropriate cell identity within leaf primorida, the small, undifferentiated plastids, called proplastids, inside them must also differentiate, usually into chloroplasts.

Many mutants lacking functional plastid-localized proteins exhibit secondary defects in leaf cell specification ((Larkin, 2014; Luesse et al., 2015; Moschopoulos et al., 2012), providing genetic evidence that normal leaf development depends upon plastid homeostasis. The integration of plastid differentiation into the process of development likely requires tightly regulated and finely tuned two-way communication between the plastid and the nucleus, including both anterograde (nucleus-to-plastid) and retrograde (plastid-to-nucleus) signaling. An increasing number of overlapping retrograde signaling pathways, triggered by developmental or environmental defects in plastid function, have been identified (Chan et al., 2015; Woodson and Chory, 2012). Numerous retrograde signals have been proposed, including intermediates in tetrapyrrole (Mochizuki et al., 2001) or isoprenoid (Xiao et al., 2012) biosynthesis, heme (Woodson et al., 2011), phosphonucleotides (Estavillo et al., 2011), reactive oxygen species (ROS) (Wagner et al., 2004) and oxidized carotenoids (Ramel et al., 2012). Despite the diversity, all these pathways and signals link a disruption in plastid homeostasis to altered nuclear gene expression (Chan et al., 2015).

One retrograde signaling pathway that may serve to connect plastid signals to shoot development is the GENOMES UNCOUPLED (GUN1) / ABA-INSENSITIVE 4 (ABI4) pathway (Fernandez and Strand, 2008; Leon et al., 2012). ABI4 is a nuclear transcription factor involved in many plant developmental pathways, including response to ABA, sugar signaling, and mitochondrial retrograde signaling (Leon et al., 2012). GUN1 is a plastid protein of unclear molecular function thought to function with ABI4 in at least two retrograde signaling pathways, one that coordinates plastid and nuclear gene expression during development, and one that respond to defects in chlorophyll biosynthesis (Cottage et al., 2010; Koussevitzky et al., 2007; Sun et al., 2011).

ROS are both byproducts of the metabolic reactions that occur within cells, and serve as important signaling molecules in plant development, stress response, and programmed cell death (Apel and Hirt, 2004). In plant cells, chloroplasts are major sources of ROS such as singlet oxygen ($^1O_2$), superoxide (O_2^-), and hydrogen peroxide (H_2O_2). Numerous studies support a role for ROS in retrograde signaling

(Barajas-Lopez Jde et al., 2013; Galvez-Valdivieso and Mullineaux, 2010; Pogson et al., 2008) and their involvement in multiple pathways including the GUN1/ABI4 pathway (Moulin et al., 2008).

We have been using an Arabidopsis mutant with constitutively osmotically stressed plastids (*msl2 msl3* (Veley et al., 2012)) as a model system to address the developmental effects of plastid dysfunction. MSL2 and MSL3 are two members of the MscS-Like family of mechanosensitive ion channels that localize to the plastid envelope and are required for normal plastid size, shape, and division site selection (Haswell and Meyerowitz, 2006; Wilson et al., 2011). By analogy to family members in bacteria (Levina et al., 1999) and plants (Hamilton et al., 2015), and based on *in vivo* experiments (Veley et al., 2012), MSL2 and MSL3 are likely to serve as osmotic "safety valves", allowing plastids to continuously maintain osmotic homeostasis during normal growth and development. In addition, *msl2 msl3* mutant plants exhibit small stature, variegated leaf color, and ruffled leaf margins. These whole-plant defects can be attributed to plastid osmotic stress, as they are suppressed by environmental and genetic manipulations that increase cytoplasmic osmolarity and draw water out of the plastid (Veley et al., 2012; Wilson et al., 2014).

Here we report a new and unexpected phenotype associated with *msl2 msl3* mutants, and establish the molecular and genetic pathways that underlie it. Our data provide evidence that plastid status is important to maintain cell identity decisions at the SAM, that plastid dysfunction promotes cell proliferation through two non-redundant pathways: one involving SAM identity genes and CK; and one involving the production of plastidic ROS, ABA, and the GUN1/ABI4 pathway.

RESULTS

msl2 msl3 double mutants develop callus at the shoot apex

When grown on solid media, *msl2 msl3* double mutant plants developed a proliferating mass of undifferentiated cells, or callus, at the apex of the plant (Fig. 1A-D). Calluses lacked pigmentation and formed translucent finger-like cellular projections across their surface. A single mass at the center of the apex, twin masses associated with the cotyledon petioles; and occasionally three masses were observed Fig. 1A-C). New green tissue was frequently observed growing out of the apical callus (white arrow, Fig. 1D).

We characterized the developmental progression of callus production in *msl2 msl3* seedlings, starting at 8 days after germination (DAG) and ending at 22 DAG for the mutant and at 16 DAG (when seedlings bolted) for the wild type (Fig. 1E, top two rows). Masses of callus tissue were apparent to the naked eye at the apex of *msl2 msl3* seedlings between 14 and 16 DAG and continued to grow in size through 22 DAG. The percent of *msl2 msl3* seedlings with callus increased to ~82% by 21 DAG (Fig. 1F); callus was not observed in any wild type plants at any developmental stage. To determine how suppression of developmental defects depended on age and developmental stage, seedlings were germinated on MS solid media and transferred to media containing 100 mM NaCl at 2, 5, 7, or 9 DAG and assessed at 21 DAG for callus formation and leaf development. Full suppression of callus formation and abnormal leaf development was only observed in seedlings transferred to solid media containing NaCl from MS at 2 DAG (Fig. 1G and H). The reason for a slight reduction in callus formation was observed in seedlings transferred from MS to MS at later stages of development is unclear. These results establish a small developmental window, after which alleviation of plastid hypoosmotic stress can no longer suppress leaf morphology defects and apical callus production in *msl2 msl3* mutants.

The converse experiment was also conducted, in which seedlings were germinated on solid media containing 82 mM NaCl and then transferred to media lacking NaCl (Fig. 1H and S1). Seedlings that were transferred to NaCl-free media at 7 and 9 DAG had wild-type true leaves and lacked apical callus, but after transfer developed leaves that exhibited the usual mutant phenotypes (Fig. S1). These observations show that plastid osmotic homoeostasis is continuously required to maintain normal leaf development.

Plastids in the SAM of *msl2 msl3* mutants are morphologically abnormal

We next characterized the morphology of developing chloroplasts and proplastids in the SAM and surrounding tissue of *msl2 msl3* mutant seedlings using transmission electron microscopy (Fig. 2A and S2B). In the *msl2 msl3* mutant, young chloroplasts were enlarged, lacked the lens shape of wild-type chloroplasts, and exhibited a disorganized developing thylakoid network (Fig. 2B-C). In agreement with previous reports (Charuvi et al., 2012), wild-type proplastids appeared as small structures (0.5-1 μm in diameter) containing rudimentary thylakoid networks of varying developmental stages, plastoglobules, and double membranes (Fig. 2F and Fig. S2A). However, in the SAM of *msl2 msl3* mutants, entities with these established features had decreased stromal density and were greatly enlarged compared to the wild type (asterisks in Fig. 2A and S2B, Fig. 2D). Many exceeded 5 μm in diameter. All were clearly bound by a double membrane (white arrow, Fig. 2E and S2C-D). These data show that the greatly enlarged phenotype of non-green plastids of the leaf epidermis (Haswell and Meyerowitz, 2006; Veley et al., 2012) extends to proplastids of the SAM.

MSL2 function is required in the SAM or leaf primordia to prevent callus production

To determine if MSL2 expression in the SAM and leaf primordia was required to prevent callus production in the *msl2 msl3* background, we examined apical callus production in *msl2 msl3* mutant plants expressing *MSL2* from the *SCARECROW (SCR)* promoter, which is expressed throughout the L1 cell layer of the meristem including the PZ and in most cells of leaf primordia (Wysocka-Diller et al., 2000). As shown in Fig. 2G, apical callus formation was fully suppressed in T2 *msl2 msl3 SCRpMSL2* lines. While these plants developed multiple sets of developmentally normal true leaves, the majority of T2 lines examined exhibited reduced stature. Thus, expression of *MSL2* in the L1 cell layer of the SAM and leaf primordia is sufficient to prevent callus formation and partially suppress other aerial tissue phenotypes.

Callus produced in *msl2 msl3* mutants is the result of an altered cytokinin: auxin ratio and requires CK perception

The production of shooty callus has been associated with increased production or availability of CKs and an imbalance in the cytokinin: auxin ratio (Frank et al., 2002; Frank et al., 2000; Lee et al., 2004). Consistent with these observations, apical callus production, dwarfing and leaf phenotypes of the *msl2 msl3* double mutant were strongly suppressed when seedlings were grown on media supplemented

with the synthetic auxin 1-naphthaleneacetic acid (NAA) (Fig. 3A, C). When *msl2 msl3* seedlings harboring the plastid marker RecA-dsRED (Haswell and Meyerowitz, 2006; Wilson et al., 2014) were grown on 2 μM NAA, no change in the large, round non-green plastid phenotype was observed (Fig. 3B), indicating that NAA treatment suppresses callus formation downstream of effects on plastid morphology. In agreement with previous data, growth on media supplemented with osmolytes fully suppressed the plastid morphology defects (Veley et al., 2012). We next measured the CK and auxin levels present in 21-day-old wild type and mutant seedlings by liquid chromatography-mass spectrometry/mass spectrometry. Trans-Zeatin-riboside levels were increased ~6.5-fold in *msl2 msl3* mutant seedlings compared to the wild type, but IAA levels were not significantly changed (Fig. 3D).

The *ARABIDOPSIS HISTIDINE KINASE (AHK)2* gene encodes one of three related histidine kinases known to function as CK receptors in Arabidopsis (Ueguchi et al., 2001; Yamada et al., 2001), and an *AHK2* loss of function mutant, *ahk2-2* (Higuchi et al., 2004) is impaired in CK-induced up-regulation of *WUS* (Gordon et al., 2009). Two independently isolated *msl2 msl3 ahk2-2* triple mutants were similar to the msl2 msl3 double with respect to leaf developmental defect (Fig. 3E), but showed a significant reduction in apical callus formation with less than 40% of seedlings developing callus (Fig. 3F). Incomplete suppression with respect to callus formation may be due to redundancy among CK receptors (Gordon et al., 2009).

To determine if feedback loops involving *WUS*, *ARRs* (Gordon et al., 2009; Schuster et al., 2014), or the meristem identity gene *STM* (Scofield et al., 2013) were mis-regulated in *msl2 msl3* seedlings, Quantitative RT-PCR was used to determine transcript levels in the aerial tissue of 7- and 21-day-old seedlings (Fig. 3G). In *msl2 msl3* mutant seedlings *WUS* transcript levels were up-regulated 5.3-fold compared to the wild type by 7 DAG (prior to visible callus development, Fig. 1E); and 4-fold by 21 DAG. *STM* expression levels were up-regulated 2.1-fold in 7-day-old *msl2 msl3* mutants, but were not distinguishable from the wild type at 21 DAG. *ARR7* and *ARR15* transcript levels were reduced in both 7 and 21 day old *msl2 msl3* mutant seedlings compared to wild type, exhibiting 2 to 2.6-fold and 3- to 6-fold decreases, respectively. Transcriptional repression is specific to *ARR7* and *ARR15*, as transcript levels of two other A-type *ARR* genes were either unchanged (*ARR4*) or slightly elevated (*ARR5*) in *msl2 msl3* mutant seedlings compared to wild type.

Preventing Pro biosynthesis results in a dramatic increase in callus formation and CK levels in the *msl2 msl3* background

It was not obvious how the constitutive plastid osmotic stress experienced by *msl2 msl3* mutants might elicit these effects, but we reasoned that the hyper-accumulation of solutes previously observed in *msl2 msl3* mutants, especially the compatible osmolyte Proline (Pro) (Wilson et al., 2014), might be responsible. To test this hypothesis, we crossed the *pyrroline-5-carboxylate synthetase1-1* (*p5cs1-4*) lesion into the *msl2 msl3* mutant background. P5CS1 catalyzes the primary step in the inducible production of Pro (Verslues and Sharma, 2010), and stress-induced Pro levels are low in this mutant (Szekely et al., 2008). *msl2 msl3 p5cs1-4* triple mutant seedlings exhibited larger calluses than the *msl2 msl3* double, frequently forming multiple calluses (Figs. 1E, and S3A), and formation was more observed at earlier stages of development in *msl2 msl3 p5cs1-4* triple compared to *msl2 msl3* double mutants (Fig. 4A, light blue bars)—at 14 DAG over 40% of triple mutant seedlings had visible callus, while only 15% of the double *msl2 msl3* mutants did (Fig. 4A, light blue bars). Neither wild type nor *p5cs1-4* single mutants produced callus at any time point. A different mutant allele of *P5CS1*, *p5cs1-1* (Szekely et al., 2008), also enhanced callus formation in the *msl2 msl3* background (Fig. S3B-C). In addition *msl2 msl3 p5cs1-4* triple mutants exhibited 7 times more trans-Zeatin-riboside levels than *msl2 msl3* mutants (Fig. 3D). Supplementing growth media had no effect on callus production in *msl2 msl3* double or *msl2 msl3 p5cs1-4* triple mutants at any time point (Fig. 4A), even though *msl2 msl3 p5cs1-4* triple mutant seedlings grown on 20 mM Pro for 21 DAG contained as much Pro as the *msl2 msl3* double (Fig. 4B).

The process of Pro biosynthesis is a key reductive pathway that helps maintain cellular redox homeostasis (Szabados and Savoure, 2010), and could function to reduce callus production in the *msl2 msl3* mutant background if ROS accumulation were involved. To characterize the levels and localization of ROS in *msl2 msl3* double and *msl2 msl3 p5cs1-4* triple mutants, 7-, 14-, and 21-day-old mutant and wild-type seedlings were stained with 3, 3 diaminobenzidine (DAB) to detect hydrogen peroxide (H_2O_2) or nitroblue tetrazolium (NBT) to detect superoxide (O_2^-) (Fig. 4C). Both double and triple mutants accumulated high levels of H_2O_2 and O_2^- in the SAM region relative to the *p5cs1-4* single mutant or the wild type. Precipitate was visible earlier in the *msl2 msl3 p5cs1-4* triple mutant (by 14 DAG compared to 21 DAG in the in the double *msl2 msl3* mutant). Quantitation of H_2O_2 levels using an Amplex Red enzyme assay at these same time points showed consistent accumulation of H_2O_2 in the double and triple mutants, rising to nearly three-fold over wild type by 21 DAG (Fig. 4D). Levels of formazan, the product of NBT reduction by O_2^-, increased in *msl2 msl3* and *msl2 msl3 p5cs1-4* to more than 2.5-fold above wild-type levels at 21 DAG (Fig. 4E). Calluses generated by incubating *Arabidopsis thaliana* Col-*0* root explants on Callus Inducing Media also showed strong NBT staining in

areas of cell proliferation (Fig. S4), providing evidence that ROS accumulation may be a general feature of callus tissue (Lee et al., 2004).

The accumulation of superoxide in response to plastid hypo-osmotic stress is required for callus formation in the *msl2 msl3* background.

In plastids, the photoreduction of molecular O_2 generates O_2^-, which is then rapidly converted into H_2O_2 by plastid-localized superoxide dismutase enzymes (Asada, 2006). To determine if plastid osmotic stress and the accumulation of O_2^- at the apex of *msl2 msl3* double and *msl2 msl3 p5cs1-4* triple mutants play causative roles in callus formation, plants were germinated on or transferred to solid media supplemented with 82 mM NaCl or with TEMPOL (a O_2^- scavenger) at 3 or 7 DAG and stained with NBT at 21 DAG. Growth on media containing NaCl suppressed O_2^- accumulation in *msl2 msl3* double and *msl2 msl3 p5cs1-4* triple mutant seedlings (Fig. 5A), completely prevented callus formation (Fig. 5B), suppressed defects in non-green plastid morphology (Fig. 5C) and leaf morphology (Fig. 5A). Thus, plastid osmotic stress is responsible for O_2^- accumulation as well as callus formation in *msl2 msl3* and *msl2 msl3 p5cs1-4* mutants. Consistent with Fig. 1H, growth on NaCl suppressed callus formation and ROS accumulation only if supplied prior to 7 DAG.

Growth on TEMPOL-containing media successfully prevented the accumulation of O_2^- in the SAM of *msl2 msl3* and *msl2 msl3 p5cs1-4* mutants, regardless of seedling age at time of application (Fig. 5A), but did not affect plastid morphology (Fig, 5C) nor leaf morphology defects (Fig. 5A). Treating double and triple mutant seedlings with TEMPOL at all developmental stages partially suppressed callus formation (Fig. 5C). Less than 40% of double mutant seedlings exhibited apical calluses when grown in the presence of TEMPOL, compared to > 90% when grown on MS without TEMPOL. TEMPOL-mediated callus suppression is thus independent or downstream of the developmental window in which addition of osmotic support must be provide for complete suppression of aerial phenotypes (Figs 1H and 5A-B).

A complementary genetic approach to suppressing O_2^- accumulation in the plastid was taken by over-expressing wild type or miR398-resistant forms of the chloroplast-localized Cu/Zn Superoxide Dismutase CSD2 (Kliebenstein et al., 1998; Sunkar et al., 2006) in the *msl2 msl3* mutant background. The percentage of seedlings with visible apical callus at 21 DAG was decreased to 50% or less in six independent T2 lines segregating either wild-type (*CSD2*, lines #2, #4, and #7) or miR398 resistant (*mCSD2*, lines #1, #3, #5) *CSD2* over-expression constructs (Fig. 5D). Approximately 50% of T2

seedlings showed strong O_2^- accumulation by NBT staining, which was localized to developing callus, compared to 90% of *msl2 msl3* seedlings (Fig. 5E). 15-30% of seedlings in the CDS2 over-expression lines exhibited both low levels of O_2^- accumulation at their shoot apex and did not develop callus; less than 5% of *msl2 msl3* seedlings had these characteristics. Over-expression of *CSD2* did not suppress abnormal leaf development (Fig. 5F).

Callus production requires ABA biosynthesis, ABI4 and GUN1

As *msl2 msl3* double mutants exhibit increased levels of ABA and up-regulation of ABA biosynthesis genes (Wilson et al., 2014), we hypothesized that a pathway involving the hormone ABA and the GUN1 and ABI4 gene products might account for the pleiotropic defects in the *msl2 msl3* mutant (Koussevitzky et al., 2007; Zhang et al., 2013). Indeed, callus formation and leaf development defects were strongly suppressed in the triple mutant, with only ~20% of *msl2 msl3 aba2-1* seedlings developing callus at the shoot apex by 21 DAG (Fig. 6A, B). Similar suppression of *msl2 msl3* aerial defects was observed in four other independently isolated *msl2 msl3 aba2-1* triple mutant lines. The *msl2 msl3 aba2-1* triple mutant accumulated trans-Zeatin-riboside to levels similar to the *msl2 msl3* double mutant (Fig. 3D), suggesting that ABA and CK promote callus formation through independent pathways.

To test if GUN1 is involved in the perception of signals generated by plastid osmotic stress, we crossed the *gun1-9* (Koussevitzky et al., 2007) allele into the *msl2 msl3* mutant background and analyzed the offspring of a single *msl2 msl3 gun1-2 (+/-)* mutant plant. Out of 30 seedlings, 7 triple *msl2 msl3 gun1-9* seedlings were identified by PCR genotyping. None of the seven seedlings formed apical callus when grown on solid media, whereas sibling *msl2 msl3 gun1-9* (+/-) seedlings were indistinguishable from *msl2 msl3* double mutants (Fig. 6C). In addition, all seven *msl2 msl3 gun1-9* triple mutant siblings produced larger, greener, and more normally shaped true leaves than their *msl2 msl3* and *msl2 msl3 gun1-9+/1* siblings.

The strong *abi4-1* allele (Finkelstein et al., 1998) was also introduced into the *msl2 msl3* background, and *msl2 msl3 abi4-1* mutants also exhibited reduced apical callus formation; only ~26% of *msl2 msl3 abi4-1* seedlings from two independently isolated lines developed callus (Fig. 6B). Neither leaf developmental defects nor ROS accumulation was suppressed in the *msl2 msl3 abi4-1* mutant, and *msl2 msl3 abi4-1* seedlings stained with DAB or NBT showed a pattern of ROS accumulation similar to the *msl2 msl3* double mutant (Fig. 6D, E). These staining patterns were not observed in wild type or

abi4-1 single mutants. These results are consistent with a model wherein ABI4 functions downstream of ROS accumulation, and likely in a pathway with GUN1, to induce apical callus formation in response to plastid osmotic stress.

DISCUSSION

One of the most fundamental decisions a cell can make is whether to proliferate or to differentiate. In the plant SAM, this decision must be spatially and temporally controlled, so that cells remain in an undifferentiated, pluripotent state in the central zone of the meristem and then differentiate properly as they are recruited into organs at the PZ. Here we use the *msl2 msl3* mutant as a model system to show that, in the Arabidopsis SAM, proliferation versus differentiation signals are coordinated not only at the tissue- and cellular-level, but also at the organellar level. We further applied genetic, molecular, biochemical, and pharmacological approaches to identify two non-redundant pathways through which plastid dysfunction produces apical callus (illustrated in Fig. 7).

Plastid dysfunction results in the production of callus at the plant SAM

Plants lacking functional versions of the mechanosensitive ion channel homologs MSL2 and MSL3 robustly produce callus tissue at the apex of the plant when grown on solid media (Fig. 1). Of the large number of previously described mutants that produce callus (Ikeuchi et al., 2013), the *msl2 msl3* mutant most closely resembles plants silenced for the cell cycle inhibitor genes *KIP-RELATED PROTEIN (KRP)* (Anzola et al., 2010), the *main-like1 (mail1)* mutant when grown on sucrose (Uhlken et al., 2014), and the *N-isobutyl decanamide-hypersensitive (dhm1)* mutant (Pelagio-Flores et al., 2013). Molecular complementation with *MSL2* under the control of the *SCARECROW* promoter established that MSL2/MSL3 are required only in the L1 layer of the CZ and/or PZ of the SAM to prevent callus formation (Fig. 2G) and that their function is critical during the first 5 days after germination (Fig 1G, H). The production of apical callus in the *msl2 msl3* mutant is associated with dramatically enlarged and developmentally abnormal plastids specifically in the SAM (Fig. 2A-F, S2A-D). Developmentally defective plastids were also observed in the SAM of another apical callus-producing mutant, *tumorous shoot development (tsd)1* (Frank et al., 2002).

Disrupting the CK/WUS feedback loop in the SAM leads to increased proliferation and the production of callus

msl2 msl3 mutants exhibit several previously established hallmarks of increased proliferation at the SAM, including increased levels of CK< up-regulation of the stem cell identity gene *WUSCHEL*, and down-regulation of CK signaling inhibitors (Fig. 3D, G), suggesting that plastid osmotic stress activates the CK/WUS feedback loop (Gaillochet et al., 2015) (top pathway, Fig. 7). The resulting imbalance in

the cytokinin: auxin ratio is likely to underlie callus formation in the *msl2 msl3* background, as supplementing seedlings with exogenous auxin robustly suppresses all mutant phenotypes (Fig. 3A, C) without affecting plastid osmotic stress (Fig 3B). In addition, the CK receptor AHK2 is required for efficient callus formation (Fig. 3E, F). *AHK2* is required to maintain WUS expression in the meristem in response to CK treatment in the CK/WUS feedback loop (Gordon et al., 2009).

Several previously identified callus-producing mutants in Arabidopsis and Helianthus also exhibit both up-regulated CK signaling and defects in meristem identity gene expression, including *tsd1* (Frank et al., 2002; Krupkova and Schmulling, 2009); EMB-2 (Chiappetta et al., 2006); and the *pasticcino* mutants (Faure et al., 1998; Harrar et al., 2003). These data suggest that, rather than being independent mechanisms for callus production (Ikeuchi et al., 2013), the CK-induced pathway and the meristematic identity pathway are interconnected. Furthermore, the *msl2 msl3* double mutant is the only callus-producing mutant identified to date with a primary defect in plastid-localized proteins, adding a novel regulatory aspect to these known pathways, and providing the first functional link between the CK/WUS regulatory loop and plastid retrograde signaling.

Plastid retrograde signaling is required for increased proliferation and the production of callus

Genetic lesions that reduce Pro biosynthesis significantly exacerbated callus production in the *msl2 msl3* background, an effect that can not be attributed to low levels of Pro itself (Figs. 1E, 4A, B, S3). Instead, the hyper-accumulation of ROS that results from blocking Pro biosynthesis is required (Fig. 5). Treatment with exogenous ROS scavenger TEMPOL as well as over-production of CSD2, a chloroplast-localized superoxide-scavenging enzyme, prevented or reduced callus formation. Plastid osmotic stress was required for ROS hyper-accumulation (Fig. 5A-C). In addition, the analysis of callus formation in higher order mutants established that ABA biosynthesis and the retrograde signaling proteins GUN1 and ABI4 were required for callus formation and act downstream of ROS (Fig. 6, bottom pathway in Fig. 7). Because we were able to specifically suppress callus production, ROS accumulation, and impaired leaf development by increasing cytoplasmic osmolarity in the *msl2 msl3* background, this phenotype is very unlikely to be due to a loss of specific signaling by MSL2 or MSL3.

Multiple genetic links between plastid function and cell fate in the shoot have been previously described, and are often cited as evidence for retrograde signaling (Inaba and Ito-Inaba, 2010; Lepisto and Rintamaki, 2012; Lundquist et al., 2014). Whether ROS and/or the ABA/GUN1/ABI4 retrograde signaling pathway are employed to communicate plastid dysfunction to shoot development in any of

these other mutants is not known. However, the application of pharmacological inhibitors of plastid development or function was used to demonstrate that leaf adaxial/abaxial patterning is regulated by plastid protein translation in a GUN1-dependent pathway (Tameshige et al., 2013), and the GUN1 pathway is required to facilitate the switch from leaf cell proliferation to expansion and differentiation (Andriankaja et al., 2012). Taken together with the results reported here, these data support previously proposed models wherein a variety of plastid dysfunctions are communicated to leaf development through similar or overlapping pathways that include GUN1 (Koussevitzky et al., 2007; Leon et al., 2012).

We note that only a few of the genetic or pharmacological treatments that suppressed callus formation in the *msl2 msl3* mutant also suppressed the leaf developmental defects. Growth on exogenous auxin was the only treatment to completely suppress all of the mutant phenotypes, while preventing ABA biosynthesis, ROS accumulation or GUN1/ABI4 function only partially rescued leaf defects (Figs. 6A-E). It is possible that these differences are due to genetic redundancy or to limited uptake or transport of TEMPOL. Alternatively, there may be two fundamentally different processes that respond to plastid osmotic stress in the *msl2 msl3* mutant: one that functions in the SAM during early development, and one that functions later on in the leaves. In support of the latter proposal, subjecting seedlings to mild hyperosmotic stress has been shown to prevent leaf cell proliferation (Skirycz et al., 2011).

msl2 msl3 mutants provide a functional link between the CK/WUS feedback loop and plastid retrograde signaling in controlling cell fate at the plant apex.

Our working model, illustrated in Fig. 7, is that the production of apical callus in *msl2 msl3* mutants operates through two non-redundant pathways: the CK/WUS feedback loop and a retrograde signaling pathway involving ROS, ABA, ABI4 and GUN1. While the data presented here establish that both of these pathways are required for callus formation in the *msl2 msl3* background, whether they operate completely independently or are interconnected is not yet clear. In Fig. 7, we present them as separate pathways. Support for this comes from the fact that CK levels remain elevated in the *aba2 msl2 msl3* triple mutant (Fig. 3D), indicating that ABA biosynthesis is not upstream of the CK/WUS feedback loop.

In addition to promoting meristem identity, CKs are implicated in various aspects of plastid function, including plastid division and chlorophyll biosynthesis, often through modulating the expression of nuclear-encoded plastid genes (Cortleven and Schmulling, 2015). Changes in CK levels in response

to environmental stresses known to affect chloroplast function such as drought, salinity, and temperature extremes (Dobra et al., 2010; Kudoyarova et al., 2007; Nishiyama et al., 2011; Pospisilova et al.) have been documented. Additionally, CKs have been shown to preserve chloroplast integrity during leaf senescence by inducing protective antioxidant mechanisms (Prochazkova et al., 2008). Recent work has even provided a link between CK signaling and high light-induced photoinhibition (Cortleven et al., 2014). Thus, the work reported here contributes to a growing body of research suggesting that CKs are involved in stress-response and retrograde signaling pathways.

We speculate that two-way communication between plastids and cell fate decisions is essential to coordinate the developmental and functional state of the plastid with that of the cell within which it resides, and that it therefore necessarily involves multiple pathways. These results add yet another layer of complexity to the many regulatory pathways and feedback loops that govern dynamic cell identity decision-making at the plant shoot apex, and provide a foundation for future investigation into the relationship between meristem identity and plastid homeostasis in the SAM.

MATERIALS AND METHODS

Arabidopsis (*Arabidopsis thaliana*) Mutants

The *aba2-1* (CS156), *abi4-1* (CS8104), *p5cs1-4* (SALK_063517), *p5cs1-1* (SALK_058000), *ahk2-2* (SALK_052531), *gun1-9*, and *msl2-3* alleles are in the Columbia-*0* background. The *msl3-1* allele is in the Wassilewskija background (Haswell and Meyerowitz, 2006). Derived cleaved-amplified polymorphic sequence genotyping (Neff et al., 1998) of the *gun1-9* allele was performed using oligos CGAACGACGAAAGATTGTGAGGAGGGTCT and CCTGCAAGCATTCAGAATCGCTGAAAAAGG, digesting with PstI. The *abi4-1* allele was similarly genotyped with oligos TCAATCCGATTCCACCACCGAC and CCACTTCCTCCTTGTTCCTGC, digesting with NlaI. PCR genotyping of *msl*, *p5cs1*, and *aba2-1* alleles was performed as described (Sharma and Verslues, 2010; Szekely et al., 2008; Wilson et al., 2011).

Plant growth

Plants were grown on full-strength Murashige and Skoog (MS) medium (pH 5.7; Caisson Labs) with 0.8% (w/v) agar (Caisson Labs). NaCl, L-Pro (Sigma) and TEMPOL (Sigma) were added before autoclaving. For transfer assays, seed was surface-sterilized, sown on nylon mesh strips overlaid on 1X MS or 1X MS + 82 mM NaCl, and stratified for 2 d at 4°C before growth and transfer as described. All plants were grown at 23°C under a 16 h light regime with light fluence from 130 to 160 μmol m^{-1} s^{-1}.

Microscopy

Confocal microscopy of ds-RED labeled non-green plastids was performed as in (Wilson et al., 2014). Bright-field images were captured with an Olympus DP71 microscope digital camera and processed with DP-BSW software. Transmission electron microscopy was done on thin sections of tissue fixed for 2 h in 2% glutaraldehyde, post-fixed 90 minutes in 2% osmium tetroxide and embedded in Spurr's resin. Sections were post stained in uranyl and lead salts.

ROS detection and Quantification

Detection of H_2O_2 using 3,3'-Diaminobenzidine (DAB, Sigma) was performed as described (Wu et al., 2012) with the following modifications. Whole seedlings were incubated for 2 hrs in 1 mg/ml DAB prior to vacuum infiltration, incubated in the dark for an additional 12 hrs, and then cleared with an ethanol series. An Amplex Red Hydrogen Peroxide/Peroxidase Assay Kit (Invitrogen) was used to measure H_2O_2 production in seedlings. For in vitro localization of O_2^- with Nitrotetrazolium Blue chloride (NBT; Sigma), whole seedlings were vacuum-infiltrated with 0.1% (w/v) NBT in a 10 mM potassium

phosphate buffer (pH 7.8) containing 10 mM NaN_3. After 1 hour incubation in the dark at RT seedlings were cleared with an ethanol series. Quantification of formazan levels was performed as described in (Myouga et al., 2008).

Hormone level measurements

Approximately 100 mg of plant tissue was sampled for each of three replicates, frozen in N_2(l), and stored at -80°C before being assayed. Hormone levels were quantified by liquid chromatography–mass spectrometry/mass spectrometry as in (Chen et al., 2009).

Subcloning and Transgenic lines

pENTR-MSL2 (Haswell and Meyerowitz, 2006) was used in a Gateway technology (Life Technologies) recombination reaction with pSCR:GW (Michniewicz et al., 2015) to create *pSCR:MSL2*.

Quantitative Reverse Transcription-PCR

Quantitative reverse transcription-PCR was performed as previously described (Wilson et al., 2011). Primers used for gene expression analysis of *Actin* and *ARR* genes were previously described (Wilson et al., 2014; Zhao et al., 2010). The following primer pairs were used to amplify *WUS* (GCGATGCTTATCTGGAACAT and CTTCCAGATGGCACCACTAC) and *STM* (CAAATGGCCTTACCCTTCG and GCCGTTTCCTCTGGTTTATG).

Quantification of Free Pro

Pro was assayed using a ninhydrin assay adapted to fit a 1.7-mL microcentrifuge tube format (Abraham et al., 2010).

ACKNOWLEDGEMENTS

We thank the Washington University Plant Growth Facility staff, Kelsey Kropp, and Matt Mixdorf for technical assistance. The Proteomics and Mass Spectrometry Facility of the Donald Danforth Plant Science Center performed the hormone quantification. Lucia Strader provided *abi4-1* seeds and pSCR:GW; Ramanjulu Sunkar provided pBIB-CSD2 and pBIB-mCSD2; and Jesse Woodson and Joanne Chory provided *gun1-9* seeds.

COMPETING INTERESTS

No competing interests declared.

AUTHOR CONTRIBUTIONS

Study conception and manuscript preparation, MEW, ESH; conducting the research and formal analysis, MEW, EHB; funding acquisition, ESH.

REFERENCES

Abraham, E., Hourton-Cabassa, C., Erdei, L. and Szabados, L. (2010). Methods for determination of proline in plants. *Methods Mol Biol* **639**, 317-331.

Aichinger, E., Kornet, N., Friedrich, T. and Laux, T. (2012). Plant stem cell niches. *Annual review of plant biology* **63**, 615-636.

Andriankaja, M., Dhondt, S., De Bodt, S., Vanhaeren, H., Coppens, F., De Milde, L., Muhlenbock, P., Skirycz, A., Gonzalez, N., Beemster, G. T., et al. (2012). Exit from proliferation during leaf development in Arabidopsis thaliana: a not-so-gradual process. *Developmental cell* **22**, 64-78.

Anzola, J. M., Sieberer, T., Ortbauer, M., Butt, H., Korbei, B., Weinhofer, I., Mullner, A. E. and Luschnig, C. (2010). Putative Arabidopsis transcriptional adaptor protein (PROPORZ1) is required to modulate histone acetylation in response to auxin. *Proceedings of the National Academy of Sciences of the United States of America* **107**, 10308-10313.

Apel, K. and Hirt, H. (2004). Reactive oxygen species: metabolism, oxidative stress, and signal transduction. *Annual review of plant biology* **55**, 373-399.

Asada, K. (2006). Production and scavenging of reactive oxygen species in chloroplasts and their functions. *Plant physiology* **141**, 391-396.

Barajas-Lopez Jde, D., Blanco, N. E. and Strand, A. (2013). Plastid-to-nucleus communication, signals controlling the running of the plant cell. *Biochimica et biophysica acta* **1833**, 425-437.

Barton, M. K. (2010). Twenty years on: the inner workings of the shoot apical meristem, a developmental dynamo. *Dev Biol* **341**, 95-113.

Chan, K. X., Phua, S. Y., Crisp, P., McQuinn, R. and Pogson, B. J. (2015). Learning the Languages of the Chloroplast: Retrograde Signaling and Beyond. *Annual review of plant biology*.

Charuvi, D., Kiss, V., Nevo, R., Shimoni, E., Adam, Z. and Reich, Z. (2012). Gain and loss of photosynthetic membranes during plastid differentiation in the shoot apex of Arabidopsis. *The Plant cell* **24**, 1143-1157.

Chen, Q., Zhang, B., Hicks, L. M., Wang, S. and Jez, J. M. (2009). A liquid chromatography-tandem mass spectrometry-based assay for indole-3-acetic acid-amido synthetase. *Anal Biochem* **390**, 149-154.

Chiappetta, A., Michelotti, V., Fambrini, M., Bruno, L., Salvini, M., Petrarulo, M., Azmi, A., Van Onckelen, H., Pugliesi, C. and Bitonti, M. B. (2006). Zeatin accumulation and misexpression of a class I knox gene are intimately linked in the epiphyllous response of the interspecific hybrid EMB-2 (Helianthus annuus x H. tuberosus). *Planta* **223**, 917-931.

Chickarmane, V. S., Gordon, S. P., Tarr, P. T., Heisler, M. G. and Meyerowitz, E. M. (2012). Cytokinin signaling as a positional cue for patterning the apical-basal axis of the growing Arabidopsis shoot meristem. *Proceedings of the National Academy of Sciences of the United States of America* **109**, 4002-4007.

Cortleven, A., Nitschke, S., Klaumunzer, M., Abdelgawad, H., Asard, H., Grimm, B., Riefler, M. and Schmulling, T. (2014). A novel protective function for cytokinin in the light stress response is mediated by the Arabidopsis histidine kinase2 and Arabidopsis histidine kinase3 receptors. *Plant physiology* **164**, 1470-1483.

Cortleven, A. and Schmulling, T. (2015). Regulation of chloroplast development and function by cytokinin. *Journal of experimental botany* **66**, 4999-5013.

Cottage, A., Mott, E. K., Kempster, J. A. and Gray, J. C. (2010). The Arabidopsis plastid-signalling mutant gun1 (genomes uncoupled1) shows altered sensitivity to sucrose and abscisic acid and alterations in early seedling development. *Journal of experimental botany* **61**, 3773-3786.

Dobra, J., Motyka, V., Dobrev, P., Malbeck, J., Prasil, I. T., Haisel, D., Gaudinova, A., Havlova, M., Gubis, J. and Vankova, R. (2010). Comparison of hormonal responses to heat, drought and combined stress in tobacco plants with elevated proline content. *J Plant Physiol* **167**, 1360-1370.

Endrizzi, K., Moussian, B., Haecker, A., Levin, J. Z. and Laux, T. (1996). The SHOOT MERISTEMLESS gene is required for maintenance of undifferentiated cells in Arabidopsis shoot and floral meristems and acts at a different regulatory level than the meristem genes WUSCHEL and ZWILLE. *The Plant journal : for cell and molecular biology* **10**, 967-979.

Estavillo, G. M., Crisp, P. A., Pornsiriwong, W., Wirtz, M., Collinge, D., Carrie, C., Giraud, E., Whelan, J., David, P., Javot, H., et al. (2011). Evidence for a SAL1-PAP chloroplast retrograde pathway that functions in drought and high light signaling in Arabidopsis. *The Plant cell* **23**, 3992-4012.

Faure, J. D., Vittorioso, P., Santoni, V., Fraisier, V., Prinsen, E., Barlier, I., Van Onckelen, H., Caboche, M. and Bellini, C. (1998). The PASTICCINO genes of Arabidopsis thaliana are involved in the control of cell division and differentiation. *Development* **125**, 909-918.

Fernandez, A. P. and Strand, A. (2008). Retrograde signaling and plant stress: plastid signals initiate cellular stress responses. *Curr Opin Plant Biol* **11**, 509-513.

Finkelstein, R. R., Wang, M. L., Lynch, T. J., Rao, S. and Goodman, H. M. (1998). The Arabidopsis abscisic acid response locus ABI4 encodes an APETALA 2 domain protein. *The Plant cell* **10**, 1043-1054.

Fletcher, J. C., Brand, U., Running, M. P., Simon, R. and Meyerowitz, E. M. (1999). Signaling of cell fate decisions by CLAVATA3 in Arabidopsis shoot meristems. *Science* **283**, 1911-1914.

Frank, M., Guivarc'h, A., Krupkova, E., Lorenz-Meyer, I., Chriqui, D. and Schmulling, T. (2002). Tumorous shoot development (TSD) genes are required for co-ordinated plant shoot development. *The Plant journal : for cell and molecular biology* **29**, 73-85.

Frank, M., Rupp, H. M., Prinsen, E., Motyka, V., Van Onckelen, H. and Schmulling, T. (2000). Hormone autotrophic growth and differentiation identifies mutant lines of Arabidopsis with altered cytokinin and auxin content or signaling. *Plant physiology* **122**, 721-729.

Gaillochet, C., Daum, G. and Lohmann, J. U. (2015). O cell, where art thou? The mechanisms of shoot meristem patterning. *Curr Opin Plant Biol* **23**, 91-97.

Gaillochet, C. and Lohmann, J. U. (2015). The never-ending story: from pluripotency to plant developmental plasticity. *Development* **142**, 2237-2249.

Galvez-Valdivieso, G. and Mullineaux, P. M. (2010). The role of reactive oxygen species in signalling from chloroplasts to the nucleus. *Physiologia plantarum* **138**, 430-439.

Gordon, S. P., Chickarmane, V. S., Ohno, C. and Meyerowitz, E. M. (2009). Multiple feedback loops through cytokinin signaling control stem cell number within the Arabidopsis shoot meristem. *Proceedings of the National Academy of Sciences of the United States of America* **106**, 16529-16534.

Hamilton, E. S., Jensen, G. S., Maksaev, G., Katims, A., Sherp, A. M. and Haswell, E. S. (2015). Mechanosensitive channel MSL8 regulates osmotic forces during pollen hydration and germination. *Science* **350**, 438-441.

Harrar, Y., Bellec, Y., Bellini, C. and Faure, J. D. (2003). Hormonal control of cell proliferation requires PASTICCINO genes. *Plant physiology* **132**, 1217-1227.

Haswell, E. S. and Meyerowitz, E. M. (2006). MscS-like proteins control plastid size and shape in Arabidopsis thaliana. *Current biology : CB* **16**, 1-11.

Higuchi, M., Pischke, M. S., Mahonen, A. P., Miyawaki, K., Hashimoto, Y., Seki, M., Kobayashi, M., Shinozaki, K., Kato, T., Tabata, S., et al. (2004). In planta functions of the Arabidopsis cytokinin receptor family. *Proceedings of the National Academy of Sciences of the United States of America* **101**, 8821-8826.

Ikeuchi, M., Sugimoto, K. and Iwase, A. (2013). Plant callus: mechanisms of induction and repression. *The Plant cell* **25**, 3159-3173.

Inaba, T. and Ito-Inaba, Y. (2010). Versatile roles of plastids in plant growth and development. *Plant & cell physiology* **51**, 1847-1853.

Jarvis, P. and Lopez-Juez, E. (2013). Biogenesis and homeostasis of chloroplasts and other plastids. *Nature reviews. Molecular cell biology* **14**, 787-802.

Kliebenstein, D. J., Monde, R. A. and Last, R. L. (1998). Superoxide dismutase in Arabidopsis: an eclectic enzyme family with disparate regulation and protein localization. *Plant physiology* **118**, 637-650.

Koussevitzky, S., Nott, A., Mockler, T. C., Hong, F., Sachetto-Martins, G., Surpin, M., Lim, J., Mittler, R. and Chory, J. (2007). Signals from chloroplasts converge to regulate nuclear gene expression. *Science* **316**, 715-719.

Krupkova, E. and Schmulling, T. (2009). Developmental consequences of the tumorous shoot development1 mutation, a novel allele of the cellulose-synthesizing KORRIGAN1 gene. *Plant molecular biology* **71**, 641-655.

Kudoyarova, G. R., Vysotskaya, L. B., Cherkozyanova, A. and Dodd, I. C. (2007). Effect of partial rootzone drying on the concentration of zeatin-type cytokinins in tomato (Solanum lycopersicum L.) xylem sap and leaves. *Journal of experimental botany* **58**, 161-168.

Larkin, R. M. (2014). Influence of plastids on light signalling and development. *Philosophical transactions of the Royal Society of London. Series B, Biological sciences* **369**, 20130232.

Lee, J. H., Kim, D. M., Lim, Y. P. and Pai, H. S. (2004). The shooty callus induced by suppression of tobacco CHRK1 receptor-like kinase is a phenocopy of the tobacco genetic tumor. *Plant Cell Rep* **23**, 397-403.

Leibfried, A., To, J. P., Busch, W., Stehling, S., Kehle, A., Demar, M., Kieber, J. J. and Lohmann, J. U. (2005). WUSCHEL controls meristem function by direct regulation of cytokinin-inducible response regulators. *Nature* **438**, 1172-1175.

Leon, P., Gregorio, J. and Cordoba, E. (2012). ABI4 and its role in chloroplast retrograde communication. *Frontiers in plant science* **3**, 304.

Lepisto, A. and Rintamaki, E. (2012). Coordination of plastid and light signaling pathways upon development of Arabidopsis leaves under various photoperiods. *Molecular plant* **5**, 799-816.

Levina, N., Totemeyer, S., Stokes, N. R., Louis, P., Jones, M. A. and Booth, I. R. (1999). Protection of Escherichia coli cells against extreme turgor by activation of MscS and MscL mechanosensitive channels: identification of genes required for MscS activity. *The EMBO journal* **18**, 1730-1737.

Long, J. A., Moan, E. I., Medford, J. I. and Barton, M. K. (1996). A member of the KNOTTED class of homeodomain proteins encoded by the STM gene of Arabidopsis. *Nature* **379**, 66-69.

Luesse, D. R., Wilson, M. E. and Haswell, E. S. (2015). RNA Sequencing Analysis of the msl2msl3, crl, and ggps1 Mutants Indicates that Diverse Sources of Plastid Dysfunction Do Not Alter Leaf Morphology Through a Common Signaling Pathway. *Frontiers in plant science* **6**, 1148.

Lundquist, P. K., Rosar, C., Brautigam, A. and Weber, A. P. (2014). Plastid signals and the bundle sheath: mesophyll development in reticulate mutants. *Molecular plant* **7**, 14-29.

Michniewicz, M., Frick, E. M. and Strader, L. C. (2015). Gateway-compatible tissue-specific vectors for plant transformation. *BMC Res Notes* **8**, 63.

Mochizuki, N., Brusslan, J. A., Larkin, R., Nagatani, A. and Chory, J. (2001). Arabidopsis genomes uncoupled 5 (GUN5) mutant reveals the involvement of Mg-chelatase H subunit in plastid-to-nucleus signal transduction. *Proceedings of the National Academy of Sciences of the United States of America* **98**, 2053-2058.

Moschopoulos, A., Derbyshire, P. and Byrne, M. E. (2012). The Arabidopsis organelle-localized glycyl-tRNA synthetase encoded by EMBRYO DEFECTIVE DEVELOPMENT1 is required for organ patterning. *Journal of experimental botany* **63**, 5233-5243.

Moulin, M., McCormac, A. C., Terry, M. J. and Smith, A. G. (2008). Tetrapyrrole profiling in Arabidopsis seedlings reveals that retrograde plastid nuclear signaling is not due to Mg-protoporphyrin IX accumulation. *Proceedings of the National Academy of Sciences of the United States of America* **105**, 15178-15183.

Myouga, F., Hosoda, C., Umezawa, T., Iizumi, H., Kuromori, T., Motohashi, R., Shono, Y., Nagata, N., Ikeuchi, M. and Shinozaki, K. (2008). A heterocomplex of iron superoxide dismutases defends chloroplast nucleoids against oxidative stress and is essential for chloroplast development in Arabidopsis. *The Plant cell* **20**, 3148-3162.

Neff, M. M., Neff, J. D., Chory, J. and Pepper, A. E. (1998). dCAPS, a simple technique for the genetic analysis of single nucleotide polymorphisms: experimental applications in Arabidopsis thaliana genetics. *The Plant journal : for cell and molecular biology* **14**, 387-392.

Neuhaus, H. E. and Emes, M. J. (2000). Nonphotosynthetic Metabolism in Plastids. *Annu Rev Plant Physiol Plant Mol Biol* **51**, 111-140.

Nishiyama, R., Watanabe, Y., Fujita, Y., Le, D. T., Kojima, M., Werner, T., Vankova, R., Yamaguchi-Shinozaki, K., Shinozaki, K., Kakimoto, T., et al. (2011). Analysis of cytokinin mutants and regulation of cytokinin metabolic genes reveals important regulatory roles of cytokinins in drought, salt and abscisic acid responses, and abscisic acid biosynthesis. *The Plant cell* **23**, 2169-2183.

680 **Pelagio-Flores, R., Ortiz-Castro, R. and Lopez-Bucio, J.** (2013). dhm1, an Arabidopsis mutant with
681 increased sensitivity to alkamides shows tumorous shoot development and enhanced lateral
682 root formation. *Plant molecular biology* **81**, 609-625.
683 **Pogson, B. J., Woo, N. S., Forster, B. and Small, I. D.** (2008). Plastid signalling to the nucleus and
684 beyond. *Trends Plant Sci* **13**, 602-609.
685 **Pospisilova, J., Vagner, M., Malbeck, J., Travnickova, A. and Batkova, P.** Interactions between
686 abscisic acid and cytokinins during water stress and subsequent rehydration. *Biologia*
687 *Plantarum* **49**, 533-540.
688 **Prochazkova, D., Haisel, D. and Wilhelmova, N.** (2008). Antioxidant protection during ageing and
689 senescence in chloroplasts of tobacco with modulated life span. *Cell Biochem Funct* **26**, 582-
690 590.
691 **Ramel, F., Birtic, S., Ginies, C., Soubigou-Taconnat, L., Triantaphylides, C. and Havaux, M.**
692 (2012). Carotenoid oxidation products are stress signals that mediate gene responses to
693 singlet oxygen in plants. *Proceedings of the National Academy of Sciences of the United*
694 *States of America* **109**, 5535-5540.
695 **Schaller, G. E., Bishopp, A. and Kieber, J. J.** (2015). The yin-yang of hormones: cytokinin and auxin
696 interactions in plant development. *The Plant cell* **27**, 44-63.
697 **Schoof, H., Lenhard, M., Haecker, A., Mayer, K. F., Jurgens, G. and Laux, T.** (2000). The stem cell
698 population of Arabidopsis shoot meristems in maintained by a regulatory loop between the
699 CLAVATA and WUSCHEL genes. *Cell* **100**, 635-644.
700 **Schuster, C., Gaillochet, C., Medzihradszky, A., Busch, W., Daum, G., Krebs, M., Kehle, A. and**
701 **Lohmann, J. U.** (2014). A regulatory framework for shoot stem cell control integrating
702 metabolic, transcriptional, and phytohormone signals. *Developmental cell* **28**, 438-449.
703 **Scofield, S., Dewitte, W., Nieuwland, J. and Murray, J. A.** (2013). The Arabidopsis homeobox gene
704 SHOOT MERISTEMLESS has cellular and meristem-organisational roles with differential
705 requirements for cytokinin and CYCD3 activity. *The Plant journal : for cell and molecular*
706 *biology* **75**, 53-66.
707 **Sharma, S. and Verslues, P. E.** (2010). Mechanisms independent of abscisic acid (ABA) or proline
708 feedback have a predominant role in transcriptional regulation of proline metabolism during low
709 water potential and stress recovery. *Plant, cell & environment* **33**, 1838-1851.
710 **Skirycz, A., Claeys, H., De Bodt, S., Oikawa, A., Shinoda, S., Andriankaja, M., Maleux, K., Eloy,**
711 **N. B., Coppens, F., Yoo, S. D., et al.** (2011). Pause-and-stop: the effects of osmotic stress on
712 cell proliferation during early leaf development in Arabidopsis and a role for ethylene signaling
713 in cell cycle arrest. *The Plant cell* **23**, 1876-1888.

Skoog, F. and Miller, C. O. (1957). Chemical regulation of growth and organ formation in plant tissues cultured in vitro. *Symp Soc Exp Biol* **11**, 118-130.

Sun, X., Feng, P., Xu, X., Guo, H., Ma, J., Chi, W., Lin, R., Lu, C. and Zhang, L. (2011). A chloroplast envelope-bound PHD transcription factor mediates chloroplast signals to the nucleus. *Nat Commun* **2**, 477.

Sunkar, R., Kapoor, A. and Zhu, J. K. (2006). Posttranscriptional induction of two Cu/Zn superoxide dismutase genes in Arabidopsis is mediated by downregulation of miR398 and important for oxidative stress tolerance. *The Plant cell* **18**, 2051-2065.

Szabados, L. and Savoure, A. (2010). Proline: a multifunctional amino acid. *Trends Plant Sci* **15**, 89-97.

Szekely, G., Abraham, E., Cseplo, A., Rigo, G., Zsigmond, L., Csiszar, J., Ayaydin, F., Strizhov, N., Jasik, J., Schmelzer, E., et al. (2008). Duplicated P5CS genes of Arabidopsis play distinct roles in stress regulation and developmental control of proline biosynthesis. *The Plant journal : for cell and molecular biology* **53**, 11-28.

Tameshige, T., Fujita, H., Watanabe, K., Toyokura, K., Kondo, M., Tatematsu, K., Matsumoto, N., Tsugeki, R., Kawaguchi, M., Nishimura, M., et al. (2013). Pattern dynamics in adaxial-abaxial specific gene expression are modulated by a plastid retrograde signal during Arabidopsis thaliana leaf development. *PLoS Genet* **9**, e1003655.

To, J. P., Deruere, J., Maxwell, B. B., Morris, V. F., Hutchison, C. E., Ferreira, F. J., Schaller, G. E. and Kieber, J. J. (2007). Cytokinin regulates type-A Arabidopsis Response Regulator activity and protein stability via two-component phosphorelay. *The Plant cell* **19**, 3901-3914.

Ueguchi, C., Koizumi, H., Suzuki, T. and Mizuno, T. (2001). Novel family of sensor histidine kinase genes in Arabidopsis thaliana. *Plant & cell physiology* **42**, 231-235.

Uhlken, C., Horvath, B., Stadler, R., Sauer, N. and Weingartner, M. (2014). MAIN-LIKE1 is a crucial factor for correct cell division and differentiation in Arabidopsis thaliana. *The Plant journal : for cell and molecular biology* **78**, 107-120.

Veley, K. M., Marshburn, S., Clure, C. E. and Haswell, E. S. (2012). Mechanosensitive channels protect plastids from hypoosmotic stress during normal plant growth. *Current biology : CB* **22**, 408-413.

Verslues, P. E. and Sharma, S. (2010). Proline metabolism and its implications for plant-environment interaction. *The Arabidopsis book / American Society of Plant Biologists* **8**, e0140.

Wagner, D., Przybyla, D., Op den Camp, R., Kim, C., Landgraf, F., Lee, K. P., Wursch, M., Laloi, C., Nater, M., Hideg, E., et al. (2004). The genetic basis of singlet oxygen-induced stress responses of Arabidopsis thaliana. *Science* **306**, 1183-1185.

748 **Wilson, M. E., Basu, M. R., Bhaskara, G. B., Verslues, P. E. and Haswell, E. S.** (2014). Plastid
749 osmotic stress activates cellular stress responses in Arabidopsis. *Plant physiology* **165**, 119-
750 128.
751 **Wilson, M. E., Jensen, G. S. and Haswell, E. S.** (2011). Two mechanosensitive channel homologs
752 influence division ring placement in Arabidopsis chloroplasts. *The Plant cell* **23**, 2939-2949.
753 **Woodson, J. D. and Chory, J.** (2012). Organelle signaling: how stressed chloroplasts communicate
754 with the nucleus. *Current biology : CB* **22**, R690-692.
755 **Woodson, J. D., Perez-Ruiz, J. M. and Chory, J.** (2011). Heme synthesis by plastid ferrochelatase I
756 regulates nuclear gene expression in plants. *Current biology : CB* **21**, 897-903.
757 **Wu, A., Allu, A. D., Garapati, P., Siddiqui, H., Dortay, H., Zanor, M. I., Asensi-Fabado, M. A.,**
758 **Munne-Bosch, S., Antonio, C., Tohge, T., et al.** (2012). JUNGBRUNNEN1, a reactive
759 oxygen species-responsive NAC transcription factor, regulates longevity in Arabidopsis. *The*
760 *Plant cell* **24**, 482-506.
761 **Wysocka-Diller, J. W., Helariutta, Y., Fukaki, H., Malamy, J. E. and Benfey, P. N.** (2000).
762 Molecular analysis of SCARECROW function reveals a radial patterning mechanism common
763 to root and shoot. *Development* **127**, 595-603.
764 **Xiao, Y., Savchenko, T., Baidoo, E. E., Chehab, W. E., Hayden, D. M., Tolstikov, V., Corwin, J. A.,**
765 **Kliebenstein, D. J., Keasling, J. D. and Dehesh, K.** (2012). Retrograde signaling by the
766 plastidial metabolite MEcPP regulates expression of nuclear stress-response genes. *Cell* **149**,
767 1525-1535.
768 **Yamada, H., Suzuki, T., Terada, K., Takei, K., Ishikawa, K., Miwa, K., Yamashino, T. and Mizuno,**
769 **T.** (2001). The Arabidopsis AHK4 histidine kinase is a cytokinin-binding receptor that
770 transduces cytokinin signals across the membrane. *Plant & cell physiology* **42**, 1017-1023.
771 **Zhang, Z. W., Feng, L. Y., Cheng, J., Tang, H., Xu, F., Zhu, F., Zhao, Z. Y., Yuan, M., Chen, Y. E.,**
772 **Wang, J. H., et al.** (2013). The roles of two transcription factors, ABI4 and CBFA, in ABA and
773 plastid signalling and stress responses. *Plant molecular biology* **83**, 445-458.
774 **Zhao, Z., Andersen, S. U., Ljung, K., Dolezal, K., Miotk, A., Schultheiss, S. J. and Lohmann, J. U.**
775 (2010). Hormonal control of the shoot stem-cell niche. *Nature* **465**, 1089-1092.
776 **Zurcher, E., Tavor-Deslex, D., Lituiev, D., Enkerli, K., Tarr, P. T. and Muller, B.** (2013). A robust
777 and sensitive synthetic sensor to monitor the transcriptional output of the cytokinin signaling
778 network in planta. *Plant physiology* **161**, 1066-1075.
779
780
781 **FIGURE LEGENDS**

Fig. 1. *msl2 msl3* double mutants develop callus at the shoot apex. (A-D) Bright-field images representative of phenotypes observed in 21-day-old *msl2 msl3* seedlings grown on solid media. Shooty callus is indicated with a white arrowhead in (D). (E) Representative images of callus formation over time. (F) Average percent of *msl2 msl3* seedlings with visible callus at the indicated time after germination. 5 plates of seedlings, n > 10 seedlings per plate, were analyzed per time point. (G) The average percent of *msl2 msl3* seedlings showing visible callus at 21 DAG after transfer from MS to MS (black bars) or to MS supplemented with 82 mM NaCl (grey bars) at the indicated time points. 3 plates of seedlings, n > 10 seedlings per plate, were analyzed per treatment. (F and G) Error bars = SEM. *, difference from mock treatment, $P < 0.01$ (Student's *t*-test). (H) Representative bright-field images of the aerial portion of 21-day-old seedlings scored in (G) (top row) or seedlings transferred from MS supplemented with 82 mM NaCl to MS at indicated time points (bottom row). Size bars (A-E), 1 mm, (H), 5 mm.

Fig. 2. MSL2 function is required in the PZ/CZ/SAM to prevent callus production. Transmission electron microscope (TEM) images of *msl2 msl3* mutant SAM (A) and developing chloroplasts (B-C) and proplastids (D-F) in 4-day-old wild type and *msl2 msl3* mutant seedlings. Examples of proplastids and developing chloroplasts are indicated in *msl2 msl3* mutant by asterisks and black arrowheads, respectively. Size bar = 10 μm (A-C), 1 μm (D), and 100 nm (E-F). Plastoglobules (PG), double membrane (white arrowheads), and thylakoids (double black arrowheads) are indicated. (E) Magnified region of *msl2 msl3* plastid envelope, indicated by box in D. (F) Representative bright-field images of 14-day-old *msl2 msl3* seedlings expressing the genomic version of MSL2 (*MSL2g*) or *MSL2* under the control of the *SCR* promoter. Size bar = 5 mm.

Fig. 3. Callus produced in *msl2 msl3* mutants is the result of increased CK production or signaling. (A) Representative bright-field images of seedlings grown for 21 days on solid media containing the indicated concentration of the synthetic auxin NAA. Size bar = 1 mm. (B) Confocal micrographs of non-green plastids in the first true leaf of *msl2 msl3* mutants harboring the RecA-dsRED plastid marker and grown on MS media or media containing 82 mM NaCl or 2 μM NAA. Size bar = 10 μm. (C) Percent of *msl2 msl3* mutants exhibiting callus when grown on NAA. The average of three biological replicates of ≥ 20 seedlings each is presented. (D) trans-Zeatin-riboside and IAA levels 21-day-old seedlings determined by LC MS/MS analysis. The average of three biological replicates of ≥ 30 seedlings each is presented. Error bars indicate SD, *, $P < 0.01$ (Student's *t*-test). Representative bright-field images (E) and callus production (F) of *msl2 msl3 ahk2-2* triple mutant

816 seedlings and parental lines. Size bar = 1 mm. The average of four biological replicates of ≥ 20
817 seedlings each is presented. Error bars indicate SEM, *$P < 0.01$ (Student's *t*-test). (G) Quantitative
818 RT-PCR analysis of *WUS*, *STM*, and A-type *ARR* gene expression. The average of three biological
819 replicates (two technical replicates; n ≥ 25 seedlings each) is presented. Error bars indicate SEM.
820
821 **Fig. 4. Preventing Pro biosynthesis results in a dramatic increase in callus formation in the**
822 ***msl2 msl3*** **background. (**A) Production of apical callus in *msl2 msl3* and *msl2 msl3 p5cs1-4*
823 seedlings in the presence and absence of exogenously provided Pro. The average of three biological
824 replicates is presented, *n* ≥ 25 seedlings each. Error bars represent SD. (B) Pro content of the aerial
825 tissue of mutant and wild-type seedlings grown as in (A). The average of two biological replicates
826 (each performed in triplicate; n ≥ 30 seedlings each) is presented. (A) and (B) *, difference from *msl2*
827 *msl3*, $P < 0.01$ (Student's *t*-test). (C) Images of the meristematic region of representative seedlings
828 stained with DAB or NBT. Size bar = 1 mm. Quantification of H_2O_2 content by Amplex Red (D) and O_2^-
829 production by NBT-Formazan production (E) in mutant and wild-type seedlings of indicated age. The
830 average of three biological replicates (*n* ≥ 20 seedlings each), two technical replicates each, is
831 presented in both (D) and (E). Error bars indicate SEM**. *,** difference from the wild type, $P < 0.01$
832 (Student's *t*-test). FW, fresh weight.
833
834 **Fig. 5. Hyperaccumulation of superoxide is required for callus formation in *msl2 msl3* and**
835 ***msl2 msl3 p5cs1*** **seedlings.** (A) NBT stained seedlings provided with TEMPOL or NaCl at 0, 3 or 7
836 DAG. Size bar = 1mm. (B) Callus production in double and triple mutant seedlings when grown on MS,
837 MS supplemented with 1 mM TEMPOL or MS supplemented with 82 mM NaCl. (C) Confocal
838 micrographs of non-green plastids in the first true leaf of *msl2 msl3* mutants harboring the RecA-
839 dsRED plastid marker grown on the indicated media. Size bar = 10 μm. (D) Apical callus production in
840 T2 lines segregating transgenes that over-express *CSD2* or *mCSD2*. The average of 4 biological
841 replicates (*n* ≥ 35 seedlings each replicate) is presented. Error bars indicate SD. *, difference from
842 *msl2 msl3*, $P < 0.01$ (Student's *t*-test). (E) Percent of seedlings from (D) stained with NBT
843 accumulating formazan at the shoot apex. (*n* ≥ 20 seedlings). (F) Representative bright-field images of
844 *CSD2* over-expression T2 lines. Size bar = 1 mm.
845
846 **Fig. 6. Callus production requires ABA biosynthesis, GUN1 and ABI4.** (A) Representative bright-
847 field images of 21-day-old *msl2 msl3 aba2-1* seedlings with relevant parental controls. (B) Callus
848 production in higher order mutants at 21 DAG. The average of 3 biological replicates (*n* ≥ 15 seedlings
849 per replicate) is presented. Error bars indicate SEM. (C) Representative bright-field images of 21-day-

old *msl2 msl3 gun1-9* (+/-) and *msl2 msl3 gun1-9* (-/-) siblings at 21 DAG. (D) *msl2 msl3 abi4-1* Representative bright-field images of 21-day-old *msl2 msl3 abi4-1* seedlings with relevant parental controls. (E) Representative images of 21-day-old seedlings of the indicated genotypes stained with DAB or NBT. Size bar = 1 mm.

Fig. 7. Working Model. These results are consistent with a working model wherein plastid osmotic stress impacts both a feedback loop regulating cell proliferation in the shoot apical meristem (SAM) (based on (Gaillochet et al., 2015) and a plastid ROS-dependent retrograde signaling pathway (Leon et al., 2012). Plastid dysfunction leads to increased proliferation at the SAM and the production of callus through increased CK levels and *WUS* expression and through an unknown nuclear transcription program triggered by GUN1, ABA, and ABI4.

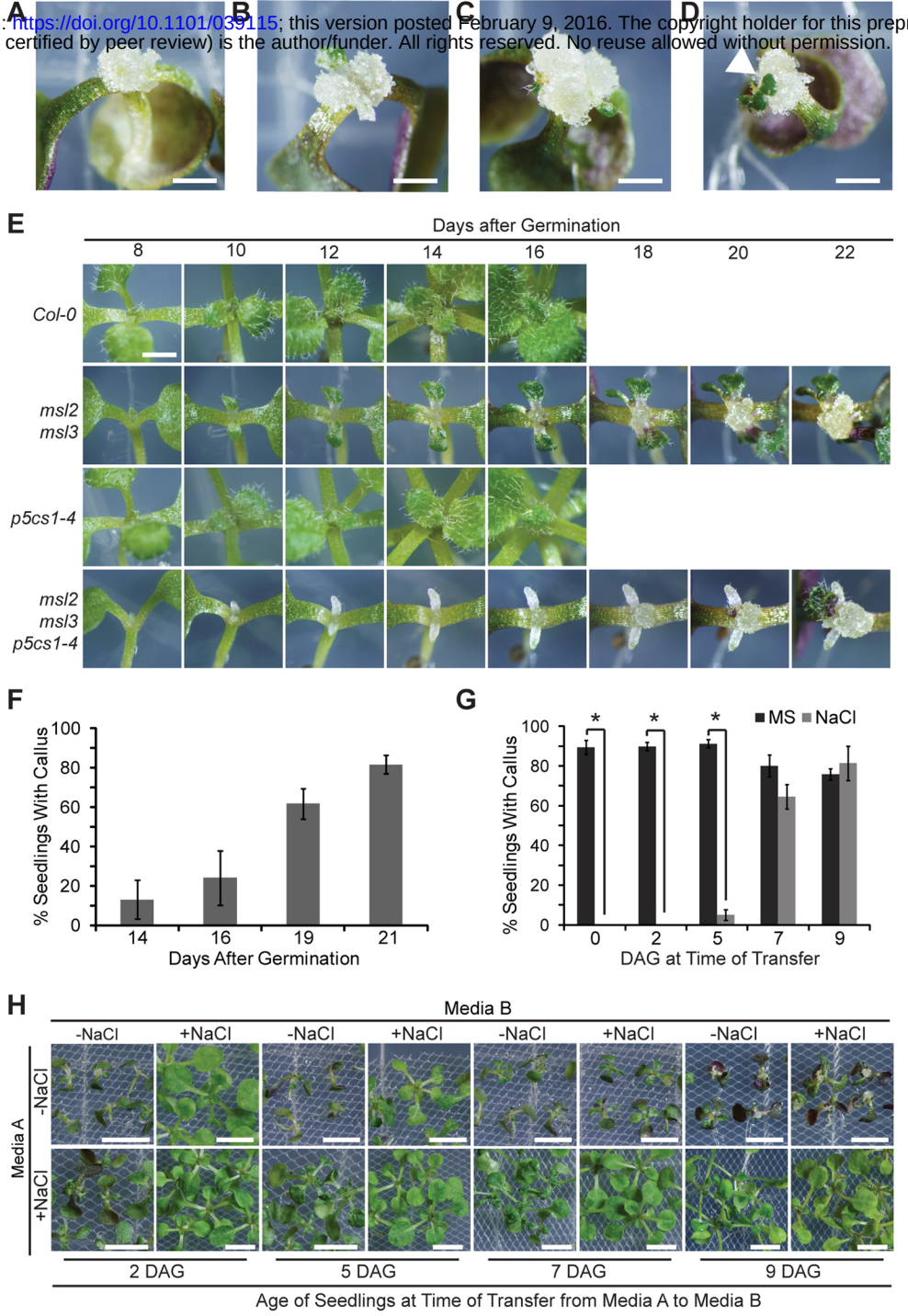

Fig. 1. *msl2 msl3* double mutants develop callus at the shoot apex. (A-D) Bright-field images representative of phenotypes observed in 21-day-old *msl2 msl3* seedlings grown on solid media. Shooty callus is indicated with a white arrowhead in (D). (E) Representative images of callus formation over time. (F) Average percent of *msl2 msl3* seedlings with visible callus at the indicated time after germination. 5 plates of seedlings, n > 10 seedlings per plate, were analyzed per time point. (G) The average percent of *msl2 msl3* seedlings showing visible callus at 21 DAG after transfer from MS to MS (black bars) or to MS supplemented with 82 mM NaCl (grey bars) at the indicated time points. 3 plates of seedlings, n > 10 seedlings per plate, were analyzed per treatment. (F and G) Error bars = SEM. *, difference from mock treatment, $P < 0.01$ (Student's *t*-test). (H) Representative bright-field images of the aerial portion of 21-day-old seedlings scored in (G) (top row) or seedlings transferred from MS supplemented with 82 mM NaCl to MS at indicated time points (bottom row). Size bars (A-E), 1 mm, (H), 5 mm.

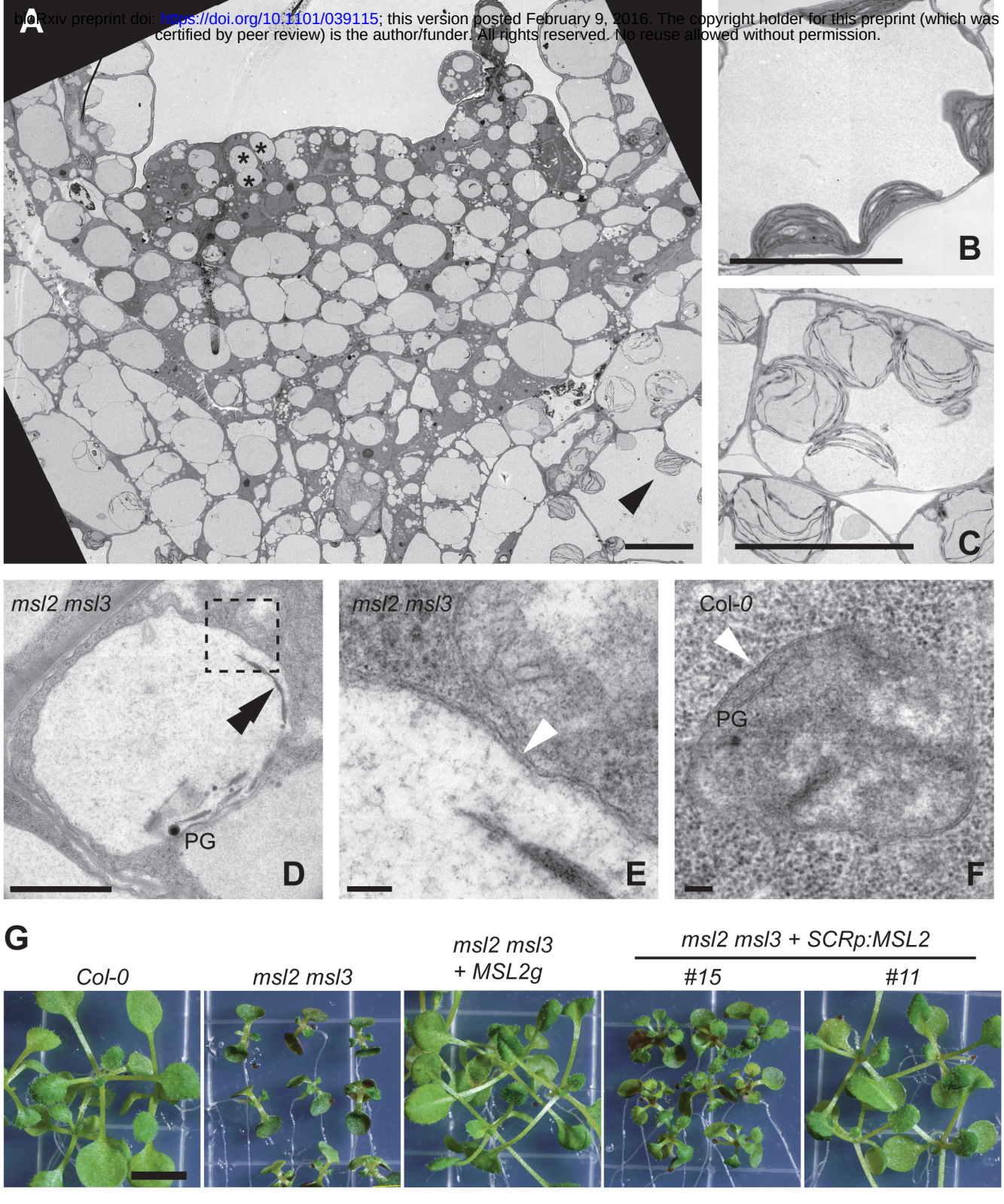

Fig. 2. MSL2 function is required in the PZ/CZ/SAM to prevent callus production. Transmission electron microscope (TEM) images of *msl2 msl3* mutant SAM (A) and developing chloroplasts (B-C) and proplastids (D-F) in 4-day-old wild type and *msl2 msl3* mutant seedlings. Examples of proplastids and developing chloroplasts are indicated in *msl2 msl3* mutant by asterisks and black arrowheads, respectively. Size bar = 10 μm (A-C), 1 μm (D), and 100 nm (E-F). Plastoglobules (PG), double membrane (white arrowheads), and thylakoids (double black arrowheads) are indicated. (E) Magnified region of *msl2 msl3* plastid envelope, indicated by box in D. (F) Representative bright-field images of 14-day-old *msl2 msl3* seedlings expressing the genomic version of MSL2 (*MSL2g*) or *MSL2* under the control of the *SCR* promoter. Size bar = 5 mm.

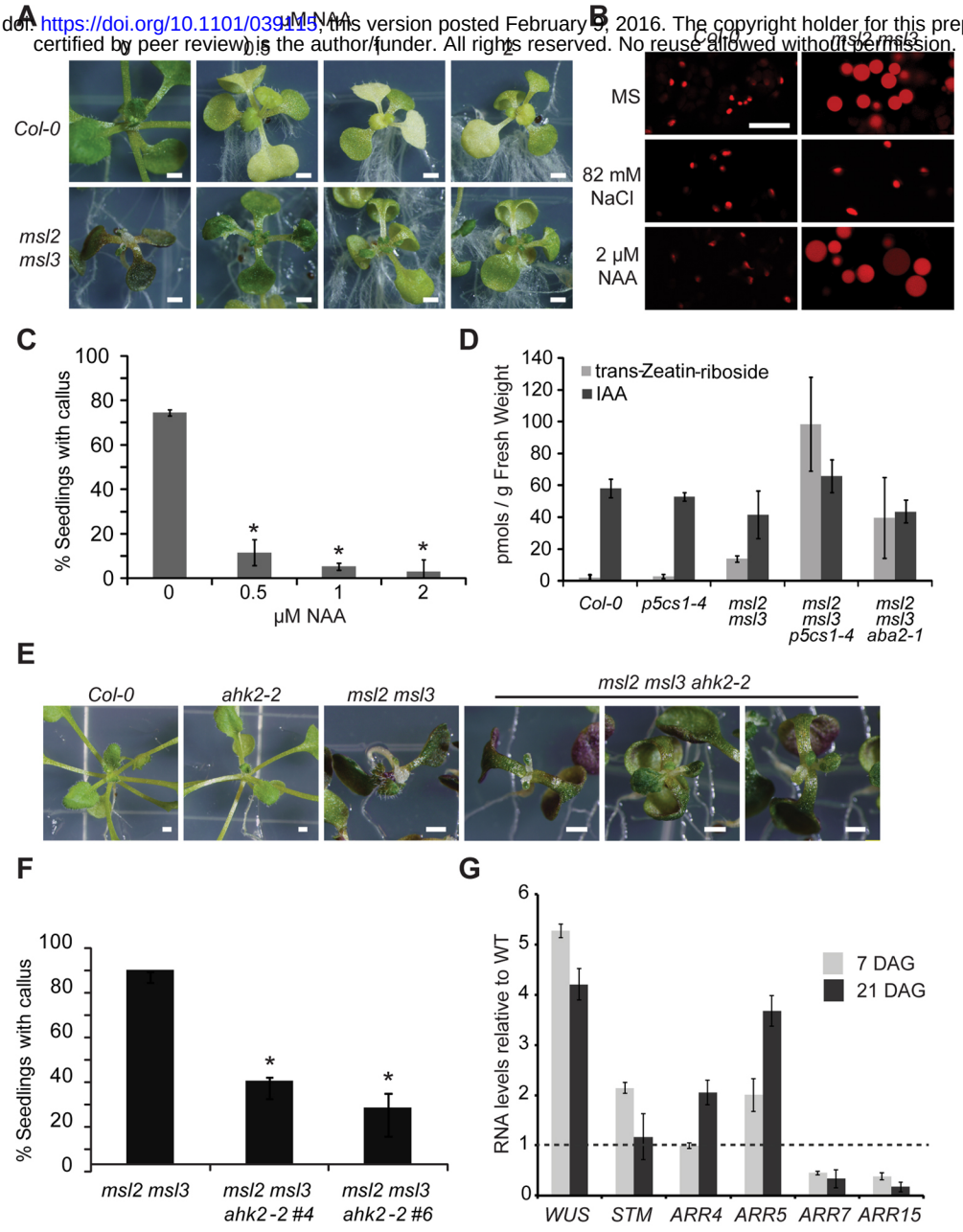

Fig. 3. Callus produced in *msl2 msl3* mutants is the result of increased CK production or signaling. (A) Representative bright-field images of seedlings grown for 21 days on solid media containing the indicated concentration of the synthetic auxin NAA. Size bar = 1 mm. (B) Confocal micrographs of non-green plastids in the first true leaf of *msl2 msl3* mutants harboring the RecA-dsRED plastid marker and grown on MS media or media containing 82 mM NaCl or 2 μM NAA. Size bar = 10 μm. (C) Percent of *msl2 msl3* mutants exhibiting callus when grown on NAA. The average of three biological replicates of ≥ 20 seedlings each is presented. (D) trans-Zeatin-riboside and IAA levels 21-day-old seedlings determined by LC MS/MS analysis. The average of three biological replicates of ≥ 30 seedlings each is presented. Error bars indicate SD, *, $P < 0.01$ (Student's *t*-test). Representative bright-field images (E) and callus production (F) of *msl2 msl3 ahk2-2* triple mutant seedlings and parental lines. Size bar = 1 mm. The average of four biological replicates of ≥ 20 seedlings each is presented. Error bars indicate SEM, *$P < 0.01$ (Student's *t*-test). (G) Quantitative RT-PCR analysis of *WUS*, *STM*, and A-type *ARR* gene expression. The average of three biological replicates (two technical replicates; n ≥ 25 seedlings each) is presented. Error bars indicate SEM.

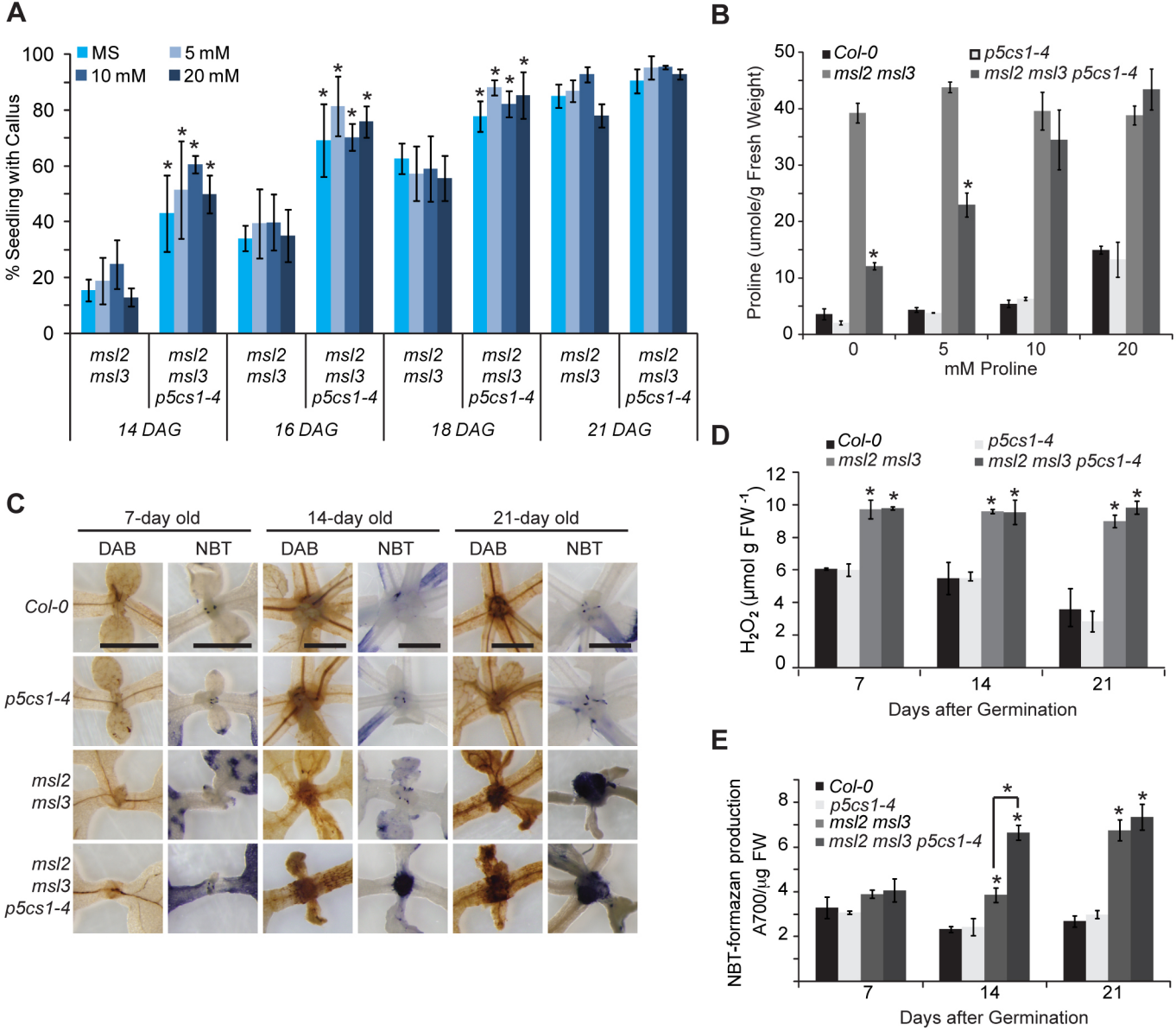

Fig. 4. Preventing Pro biosynthesis results in a dramatic increase in callus formation in the *msl2 msl3* background. (A) Production of apical callus in *msl2 msl3* and *msl2 msl3 p5cs1-4* seedlings in the presence and absence of exogenously provided Pro. The average of three biological replicates is presented, $n \geq 25$ seedlings each. Error bars represent SD. (B) Pro content of the aerial tissue of mutant and wild-type seedlings grown as in (A). The average of two biological replicates (each performed in triplicate; n ≥ 30 seedlings each) is presented. (A) and (B) *, difference from *msl2 msl3*, $P < 0.01$ (Student's *t*-test). (C) Images of the meristematic region of representative seedlings stained with DAB or NBT. Size bar = 1 mm. Quantification of H_2O_2 content by Amplex Red (D) and O_2^- production by NBT-Formazan production (E) in mutant and wild-type seedlings of indicated age. The average of three biological replicates ($n \geq 20$ seedlings each), two technical replicates each, is presented in both (D) and (E). Error bars indicate SEM. *, difference from the wild type, $P < 0.01$ (Student's *t*-test). FW, fresh weight.

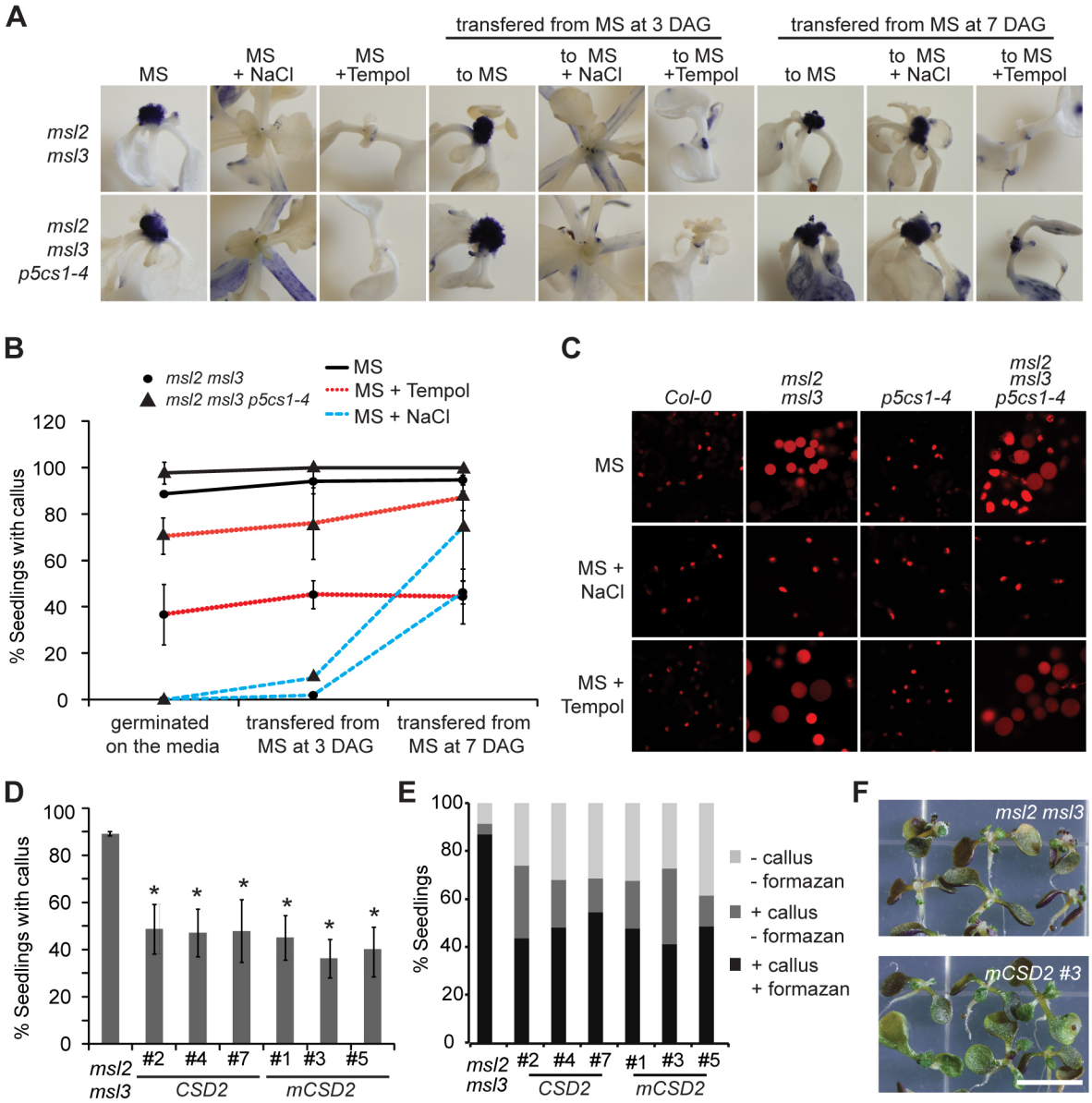

Fig. 5. Hyperaccumulation of superoxide is required for callus formation in *msl2 msl3* and *msl2 msl3 p5cs1* seedlings. (A) NBT stained seedlings provided with TEMPOL or NaCl at 0, 3 or 7 DAG. Size bar = 1mm. (B) Callus production in double and triple mutant seedlings when grown on MS, MS supplemented with 1 mM TEMPOL or MS supplemented with 82 mM NaCl. (C) Confocal micrographs of non-green plastids in the first true leaf of *msl2 msl3* mutants harboring the RecA-dsRED plastid marker grown on the indicated media. Size bar = 10 μm. (D) Apical callus production in T2 lines segregating transgenes that over-express *CSD2* or *mCSD2*. The average of 4 biological replicates ($n \geq 35$ seedlings each replicate) is presented. Error bars indicate SD. *, difference from *msl2 msl3*, $P < 0.01$ (Student's *t*-test). (E) Percent of seedlings from (D) stained with NBT accumulating formazan at the shoot apex. ($n \geq 20$ seedlings). (F) Representative bright-field images of *CSD2* over-expression T2 lines. Size bar = 1 mm.

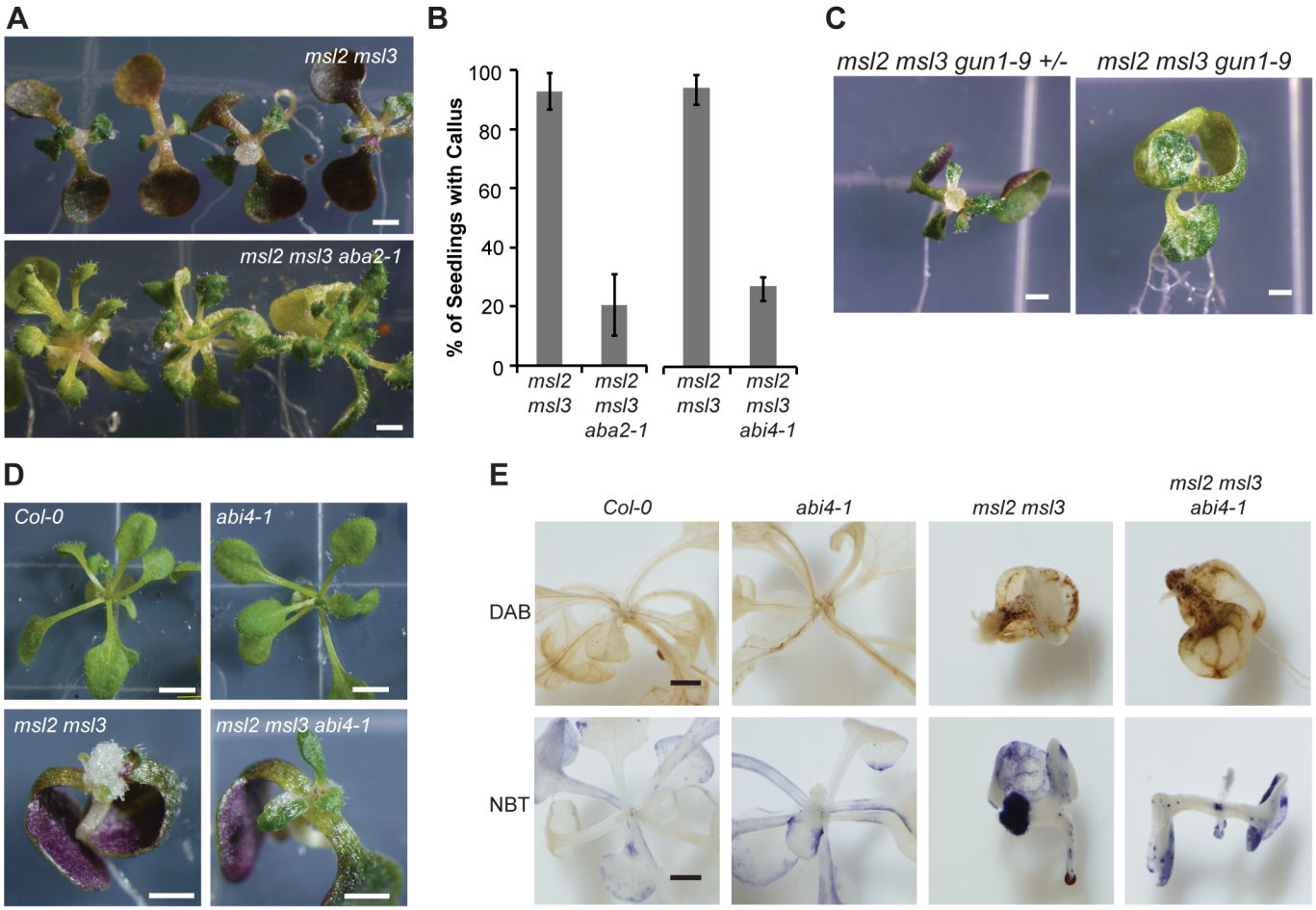

Fig. 6. Callus production requires ABA biosynthesis, GUN1 and ABI4. (A) Representative bright-field images of 21-day-old *msl2 msl3 aba2-1* seedlings with relevant parental controls. (B) Callus production in higher order mutants at 21 DAG. The average of 3 biological replicates ($n \geq 15$ seedlings per replicate) is presented. Error bars indicate SEM. (C) Representative bright-field images of 21-day-old *msl2 msl3 gun1-9* (+/-) and *msl2 msl3 gun1-9* (-/-) siblings at 21 DAG. (D) *msl2 msl3 abi4-1* Representative bright-field images of 21-day-old *msl2 msl3 abi4-1* seedlings with relevant parental controls. (E) Representative images of 21-day-old seedlings of the indicated genotypes stained with DAB or NBT. Size bar = 1 mm.

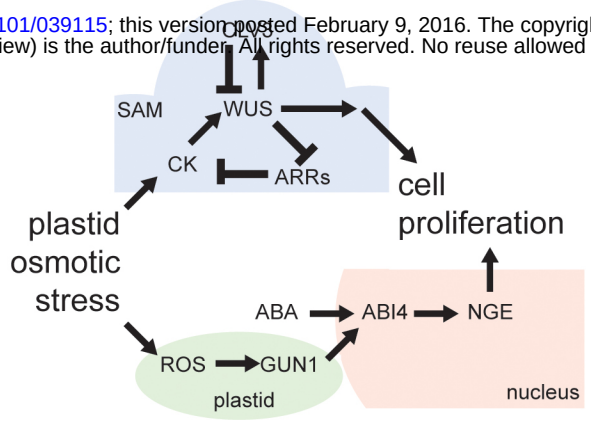

Fig. 7. Working Model. These results are consistent with a working model wherein plastid osmotic stress impacts both a feedback loop regulating cell proliferation in the shoot apical meristem (SAM) (based on (Gaillochet et al., 2015) and a plastid ROS-dependent retrograde signaling pathway (Leon et al., 2012). Plastid dysfunction leads to increased proliferation at the SAM and the production of callus through increased CK levels and *WUS* expression and through an unknown nuclear transcription program triggered by GUN1, ABA, and ABI4.